PHYSICAL REVIEW B VOLUME 44, NUMBER 23 15 DECEMBER 1991-I

# Transverse magnetotunneling in $Al_xGa_{1-x}As$ capacitors. III. Tunneling into interface Landau states in $n^+$-type GaAs

T. W. Hickmott
*IBM Research Division, Thomas J. Watson Research Center, Yorktown Heights, New York 10598*

(Received 18 April 1991)

Current-voltage ($I$-$V$) characteristics of two $n^-$-type GaAs–undoped $Al_xGa_{1-x}As$–$n^+$-type GaAs ($Al_xGa_{1-x}As$) capacitors have been measured in transverse magnetic fields $B$, in which $B$ is parallel to the capacitor interfaces and perpendicular to the tunnel current $J$. Structure is observed in $I$-$V$ curves due to tunneling into interface Landau states at the $Al_xGa_{1-x}As/(n^+$-type GaAs) interface. Capacitance-voltage curves of the $Al_xGa_{1-x}As$ capacitors are used to correct the measured voltage spacing of extrema in derivatives of $I$-$V$ curves for band bending in the $n^+$-type GaAs gate electrode and to derive the spacing of Landau states at the $Al_xGa_{1-x}As/(n^+$-type GaAs) interface. From the spacing of Landau states, cyclotron effective masses for electrons at the $Al_xGa_{1-x}As/(n^+$-type GaAs) interface are obtained that vary between $\sim 0.042$ for electrons with energies less than the band discontinuity and 0.10 for electrons that have energies that are much larger than the band discontinuity. The results agree qualitatively with the calculations of Johnson and MacKinnon [J. Phys. C **21**, 3091 (1988)] of the nature of magnetic interface states between materials of different effective mass.

## INTRODUCTION

Measurements of transverse magnetotunneling in single-barrier semiconductor heterostructures have shown complex structure in current-voltage ($I$-$V$) curves due to magnetoquantized states in the degenerately doped $n^+$-type semiconductor into which electrons tunnel.[1–5] There have been a number of theoretical papers that calculate structure in transverse magnetotunneling curves,[6–9] but only limited experimental results have been published. In this paper, detailed results on transverse magnetotunneling are presented for two $Al_xGa_{1-x}As$ capacitors in order to show differences in behavior that can occur for samples with similar basic structures.

A schematic energy diagram of the $n^-$-type GaAs–undoped $Al_xGa_{1-x}As$–$n^+$-type GaAs capacitors used in Ref. 1 and in the present work is shown in Fig. 1(a). Undoped $Al_xGa_{1-x}As$ serves as the capacitor dielectric, and single-crystal GaAs as the electrodes. $E_C$ shows the bottom of the conduction band; $E_{FS}$ and $E_{FG}$ show the position of the Fermi level in substrate and gate, respectively. In Refs. 2–5 the basic structure is similar but the semiconductor electrodes are $n$-type (In,Ga)As and the dielectric layer is undoped InP.

When a positive gate voltage $V_G$ is applied, an accumulation layer forms on the $n^-$-type GaAs substrate. Electrons tunnel from the two-dimensional electron gas (2DEG) of the accumulation layer into the $n^+$-type GaAs gate. For longitudinal magnetotunneling the magnetic field $B$ is perpendicular to the accumulation layer and parallel to the tunneling current $J$. $I$-$V$ curves show structure due to the formation of Landau levels in the 2DEG of the accumulation layer.[10–12] For transverse magnetotunneling, $B$ is parallel to the capacitor interfaces and perpendicular to $J$. A parallel magnetic field

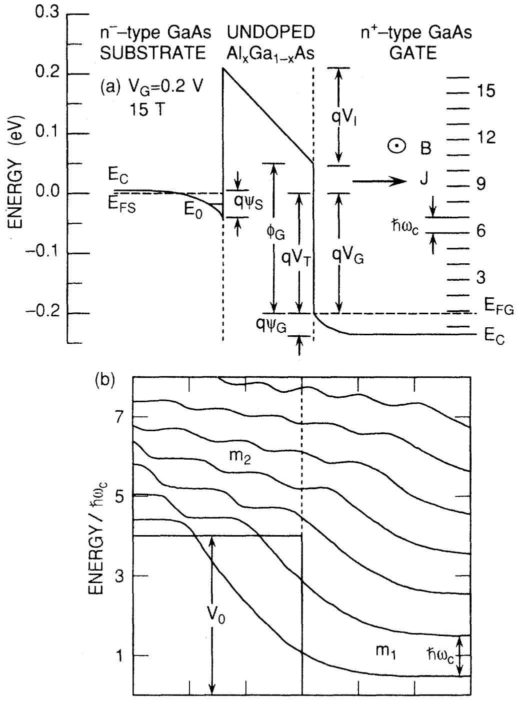

FIG. 1. (a) Schematic energy-band diagram for $n^-$-type GaAs–undoped $Al_xGa_{1-x}As$–$n^+$-type GaAs capacitor, sample $B$, biased into accumulation. Bulk Landau levels in $n^+$-type GaAs are drawn for $B = 15$ T and $m_e = 0.067m_0$. $J$ shows the direction of tunneling current, $B$ shows the direction of magnetic field. (b) Schematic Landau-level spectrum at the interface between two semiconductors with effective masses $m_1$ and $m_2$, $m_1 < m_2$. $V_0$ is the conduction-band discontinuity. Adapted from Johnson and MacKinnon (Ref. 17).

has only a small effect on the 2DEG of the accumulation layer; there is a small diamagnetic shift of $E_0$, the minimum energy of the 2DEG, but Landau levels do not form.[13]

Landau levels do, however, form in the $n^+$-type GaAs gate. As shown schematically in Fig. 1(a) there is a sequence of bulk Landau levels whose energy is given by

$$E_N = E_C + (N+1/2)\hbar\omega_c, \quad N=0,1,2\ldots \tag{1}$$

where the cyclotron energy is $\hbar\omega_c = qB\hbar/m_e$; $q$ is the electron charge, $\hbar$ is Planck's constant, $m_e$ is the effective mass of electrons in the conduction band of $n^+$-type GaAs, and $N$ is the Landau-level index. As electron states approach a barrier when the magnetic field is parallel to the barrier, the spacing between Landau levels increases.[14-17] Johnson and MacKinnon[17] have calculated the Landau level structure at the interface between two materials with a band discontinuity and with different effective masses. Figure 1(b), taken from their paper, is a schematic drawing of the behavior of Landau levels as they approach the interface. $V_0$ is the magnitude of the band discontinuity and $m_1$ and $m_2$ are the effective masses in the two materials, $m_1 < m_2$. In Fig. 1(b), energies are expressed as multiples of the cyclotron energy. The coordinate system assumes that $J$ is parallel to the $x$ axis and $B$ is parallel to the $z$ axis. Distances from the interface are expressed as the guiding center $X$, which is the classical orbit center position for magnetic interface states. $X = -(\hbar k_y)/qB$, where $k_y$ is the electron wave vector in the $y$ direction; it is given in units of the magnetic length $L = (\hbar/qB)^{1/2}$. Away from the barrier, the Landau-level spacing is $\hbar\omega_c$. If $V_0$ is infinite, the Landau-level spacing at the barrier is $2\hbar\omega_c$.[14] For finite $V_0$, the Landau-level spacing for electron energies less than $V_0$ lies between $\hbar\omega_c$ and $2\hbar\omega_c$. For electron energies greater than $V_0$ there is a complex pattern of anticrossing and level repulsion that arises from the interference of magnetic interface levels and bulk Landau levels. For electron energies much greater than $V_0$ the Landau-level spacing approaches that for bulk levels in the barrier material with electron effective mass $m_2$. The ratio of effective masses for the materials of Fig. 1(b), 0.7, approximates that at the $\mathrm{Al}_x\mathrm{Ga}_{1-x}\mathrm{As}$/GaAs interface.

Theoretical calculations have been made of transverse magnetotunneling into magnetic interface states.[6-9] For electrons tunneling from the Fermi level of the accumulation layer, both energy and transverse momentum are conserved. At constant $B$, as $V_G$ increases in Fig. 1(a), a sequence of interface states at the $\mathrm{Al}_x\mathrm{Ga}_{1-x}\mathrm{As}/(n^+$-type GaAs) interface, equivalent to classical skipping orbits, crosses the Fermi energy of electrons in the accumulation layer. Each time this happens a new channel for tunneling opens and is reflected in structure in $I$-$V$ curves.[6-8] Two distinct tunneling regimes occur in $\mathrm{Al}_x\mathrm{Ga}_{1-x}\mathrm{As}$ capacitors such as shown in Fig. 1(a). At low $V_G$, direct tunneling occurs between the two GaAs layers. When $V_G$ is somewhat greater than the band discontinuity at the $\mathrm{Al}_x\mathrm{Ga}_{1-x}\mathrm{As}/(n^+$-type GaAs) interface, Fowler-Nordheim (FN) tunneling occurs in which electrons tunnel into the conduction band of the $\mathrm{Al}_x\mathrm{Ga}_{1-x}\mathrm{As}$ layer before entering the $n^+$-type layer. The first regime corresponds to tunneling into states below the band discontinuity in Fig. 1(b); the second regime corresponds to tunneling into the complex level system above the barrier in Fig. 1(b).

This is the third paper in a series on transverse magnetotunneling in $\mathrm{Al}_x\mathrm{Ga}_{1-x}\mathrm{As}$ capacitors. In I,[18] the marked sensitivity of magnetotunneling currents to the angle $\theta$ between $B$ and $J$ when $\theta$ is close to 90° and currents are high was attributed to processes occurring in the electron source, the accumulation layer of Fig. 1(a). In II,[19] a transverse magnetic field changed the phase of electrons tunneling into the conduction band of the $\mathrm{Al}_x\mathrm{Ga}_{1-x}\mathrm{As}$ dielectric and modified structure in $I$-$V$ curves due to resonant FN tunneling. In the present paper we compare transverse magnetotunneling in two samples which differ in band discontinuity and in $\mathrm{Al}_x\mathrm{Ga}_{1-x}\mathrm{As}$ thickness. From structure in magnetotunneling curves it is possible to map the spacing of interface Landau states in $n^+$-type GaAs in both the direct and FN tunneling regimes.

## EXPERIMENT

Transverse magnetotunneling has been studied in two $\mathrm{Al}_x\mathrm{Ga}_{1-x}\mathrm{As}$ capacitors, samples $A$ and $B$, which are shown schematically in Fig. 1(a). They were grown by molecular-beam epitaxy on ⟨100⟩-oriented $n^+$-type GaAs wafers which are not shown in Fig. 1(a). Properties of the two samples are shown in Table I. The same samples were used in I and were also used for measurements of magnetic localization and magnetic freezeout in $n^-$-type GaAs.[20] Procedures for characterizing the samples are given there. $N_S$ and $N_G$ are substrate and gate dopings, respectively. $\phi_G$ is the barrier height at the $\mathrm{Al}_x\mathrm{Ga}_{1-x}\mathrm{As}/(n^+$-type GaAs) interface, derived from $I$-$V$ curves between 100 and 250 K, where thermionic emission of electrons dominates $I$-$V$ curves.[21] $\epsilon_I$ is the value of the dielectric constant of $\mathrm{Al}_x\mathrm{Ga}_{1-x}\mathrm{As}$ used to model capacitance-voltage ($C$-$V$) curves of $\mathrm{Al}_x\mathrm{Ga}_{1-x}\mathrm{As}$ capacitors. $x$, the mole fraction of AlAs in $\mathrm{Al}_x\mathrm{Ga}_{1-x}\mathrm{As}$, is derived from measurements of $\phi_G$ as well as from the nominal $\mathrm{Al}_x\mathrm{Ga}_{1-x}\mathrm{As}$ composition; $\epsilon_I$ depends on $x$. $w_{\mathrm{cp}}$ is the $\mathrm{Al}_x\mathrm{Ga}_{1-x}\mathrm{As}$ thickness used in calculating $C$-$V$ curves that match experimental $C$-$V$ curves at 1.6 K. It is estimated that $w_{\mathrm{cp}}$ is about 3.0–4.0 nm larger than the tunneling thickness of the $\mathrm{Al}_x\mathrm{Ga}_{1-x}\mathrm{As}$ layer.[19] Sample areas are $4.13\times10^{-4}$ cm$^2$. Procedures for measuring $I$-$V$ and $C$-$V$ curves have been described previously.[10,20] $I$-$V$ curves were measured at 0.001 V intervals. Magnetic-field measurements were made in a superconducting magnet with the sample immersed in pumped liquid helium.

As shown in the schematic energy diagram of Fig. 1(a), when $V_G$ is applied to an $\mathrm{Al}_x\mathrm{Ga}_{1-x}\mathrm{As}$ capacitor, it divides into three parts; $\psi_S$ is the band bending in the substrate, $\psi_G$ is the band bending in the gate, and $V_I$ is the voltage across the insulator. The energy of tunneling electrons above the conduction-band edge at the $\mathrm{Al}_x\mathrm{Ga}_{1-x}\mathrm{As}/(n^+$-type GaAs) interface is equal to $V_T$.

TABLE I. Properties of $Al_xGa_{1-x}As$ capacitors. $x$ is the AlAs mole fraction in $Al_xGa_{1-x}As$; $N_S$ is the substrate doping; $N_G$ is the gate doping; $w_{cp}$ is the $Al_xGa_{1-x}As$ thickness from C-V measurements; $\epsilon_I$ is the dielectric constant for modeling C-V curves; $V_{FB}$ is the measured flat-band voltage; $V_{SH}$ is the voltage shift for calculated and experimental C-V curves to agree; and $\phi_G$ is the activation energy for thermionic emission.

| Sample | $x$ | $N_S$ ($10^{15}$ cm$^{-3}$) | $N_G$ ($10^{18}$ cm$^{-3}$) | $w_{cp}$ (nm) | $\epsilon_I$ | $V_{FB}$ (V) | $V_{SH}$ (V) | $\phi_G$ (eV) |
|---|---|---|---|---|---|---|---|---|
| *A* | 0.40 | 1.7 | 1.0 | 23.2 | 10.8 | −0.030 | 0.034 | 0.320 |
| *B* | 0.32 | 9.0 | 1.5 | 20.0 | 11.3 | −0.045 | 0.033 | 0.263 |

If $\psi_G$ and $N_G$ are known, $V_T$ is given by

$$qV_T = qV_G + E_{FG} - q\psi_G . \qquad (2)$$

$\psi_S$, $\psi_G$, $E_{FG}$, and $V_T$ are calculated from C-V curves of $Al_xGa_{1-x}As$ capacitors. In Fig. 1(a), $V_T$ and $V_G$ are nearly equal, as are $q\psi_S$ and $E_{FG}$; this is not necessarily the case but is true for sample *B* at $V_G \sim 0.2$ V. The capacitor of Fig. 1(a) is biased into accumulation. Both samples *A* and *B* show structure in *I-V* and *C-V* curves due to Landau levels in the degenerate electron gas of the accumulation layer when *B* is perpendicular to the sample.[10]

Capacitance-voltage curves for $Al_xGa_{1-x}As$ capacitors are nearly ideal; they can be modeled by conventional semiconductor-insulator-semiconductor (*S-I-S*) theory.[22] Figure 2(a) shows an experimental *C-V* curve for sample *B* at 1.6 K and 100 kHz, and a calculated *C-V* curve using the parameters in the figure. The *C-V* curve of sample *B* can only be measured below $V_G = 0.39$ V because of high sample conductance at larger voltages. Parameters calculated from *C-V* curves can be used at larger values of $V_G$. For an ideal calculated *C-V* curve, the flat-band voltage $V_{FB}$ should equal the difference in Fermi levels between substrate and gate. $E_{FG}$ is determined from $N_G$, which, in turn, is estimated by matching the experimental and calculated capacitance as closely as possible when the $n^-$-type GaAs is in strong accumulation, $V_G \gtrsim 0.1$ V. In order to match experimental and calculated *C-V* curves, the calculated curve is shifted by $V_{SH} = 0.033$ V. Figure 2(b) shows $\psi_S$, $\psi_G$, $V_I$, and $V_T$ for sample *B* as a function of $V_G$. $V_{SH}$ is included in $E_{FG}$ in calculating $V_T$. Band bending of substrate and gate is a significant fraction of $V_G$, $\sim 0.3V_G$, when an $Al_xGa_{1-x}As$ capacitor is in strong accumulation. The *S-I-S* model used to calculate *C-V* curves does not include quantum effects in the accumulation layer. This correction should be of less importance in calculating $\psi_G$ than $\psi_S$, since the gate is in depletion for $V_G > V_{FB}$.

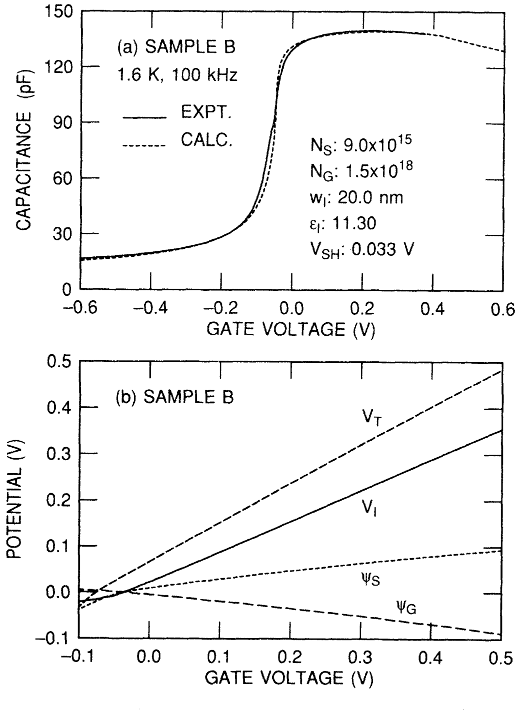

FIG. 2. (a) Experimental (solid) and calculated (dotted) capacitance-voltage curves for $Al_xGa_{1-x}As$ capacitor, sample *B*. Parameters are those used for calculated curve. Sample area: $4.13 \times 10^{-4}$ cm$^2$. (b) Dependence of $\psi_S$, $\psi_G$, $V_I$, and $V_T$ on $V_G$, calculated from theoretical *C-V* curve for sample *B*.

## RESULTS

### Tunneling in constant magnetic field

From the point of view of tunneling curves, the principal differences between samples *A* and *B* are that sample *B* is thinner, has a lower barrier height, and has a lower effective mass in the $Al_xGa_{1-x}As$ layer. These differences are reflected in the *I-V* curves of the two samples, which are shown in Fig. 3. In Fig. 3 the logarithm of current density at $\sim 2.0$ K is plotted as a function of $V_G$ for different magnetic fields parallel to the sample. The current range is about ten orders of magnitude for both samples. For $V_G \gtrsim 0.6$ V the leveling off of current in sample *B* is probably due to *IR* drops in the substrate. Structure in transverse magnetotunneling curves is not observed for $V_G \gtrsim 0.42$ V. For both samples there is a marked decrease in current at low biases as the transverse magnetic field increases. For sample *A* there is a pronounced angular dependence of *I-V* curves for $V_G \gtrsim 0.8$ V as described in I.[18] The angular dependence is much smaller for sample *B*.

Structure is visible in the *I-V* curve of sample *A* at 12 and 14 T, but is more clearly shown by plotting the difference of the logarithms of current at *B* and at 0 T, as in Fig. 4. The plot is a convenient way to show the

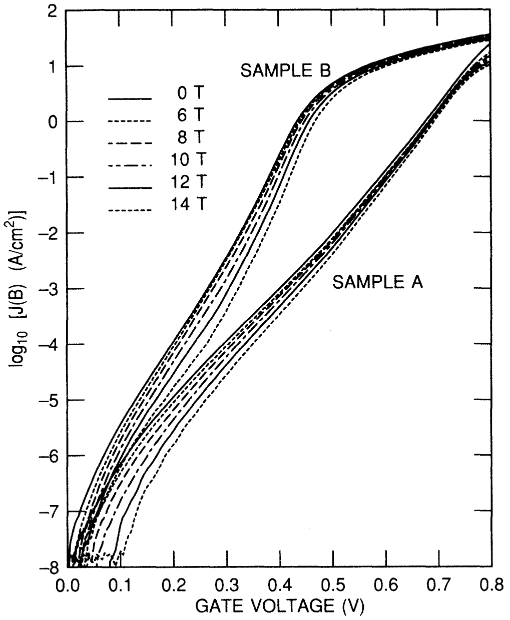

FIG. 3. Current-voltage curves of sample $A$ and sample $B$ in different transverse magnetic fields. $T\sim2.0$ K.

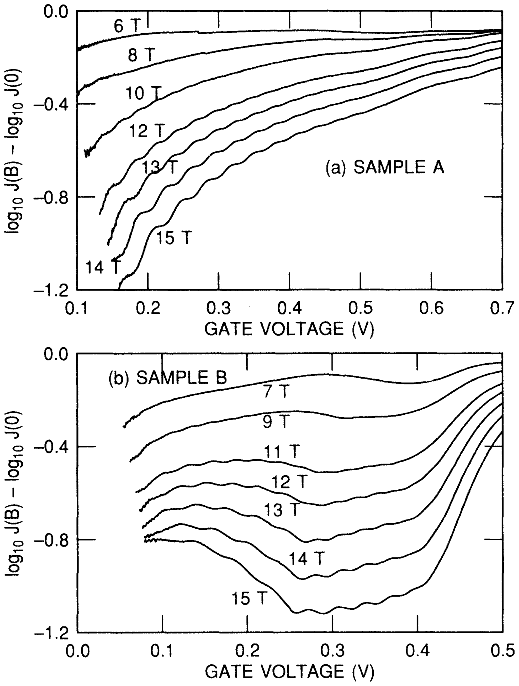

FIG. 4. (a) Dependence on $V_G$ of the difference between $\log_{10}J$ at different magnetic fields, $B$, and $\log_{10}J$ at 0 T for sample $A$ at $T=2.0$ K, and for sample $B$ at $T=2.1$ K.

effects of $B$ when the current varies by many orders of magnitude. Both samples show pronounced structure but there are differences in detail. For sample $A$, $[\log_{10}J(B)-\log_{10}J(0)]$ increases monotonically with $V_G$. For sample $B$, at high $B$, $[\log_{10}J(B)-\log_{10}J(0)]$ decreases before increasing for $V_G\gtrsim0.26$ V.

The presence of two distinct magnetotunneling regimes for sample $B$ is shown most clearly by taking the derivative of the curves of Fig. 4. Derivatives were taken numerically. Figure 5 plots $d[\log_{10}J(B)-\log_{10}J(0)]/dV$ versus $V_G$ for sample $B$ at 2.1 K. The horizontal lines in Fig. 5 correspond to the derivative equal to zero. The minimum current for derivatives was $\sim1\times10^{-10}$ A, corresponding to a current density $J\sim2.5\times10^{-7}$ A/cm$^2$. For lower currents, noise in the $I$-$V$ curves makes derivatives too noisy to use. For $11\leq B\leq15$ T and $0.1\lesssim V_G\lesssim0.24$ V, $\Delta V_m$, the spacing of either maxima or minima in derivative curves, is nearly constant. For $0.3\lesssim V_G\lesssim0.4$ V there is a second bias range in which $\Delta V_m$ is nearly constant but with a shorter period than at lower bias. The transition region is between $\sim0.24$ and $\sim0.28$ V, depending on the magnetic field. At 9 T, periodicities are barely detectable for $V_G\gtrsim0.3$ V; at 6 and 7 T, periodicities are barely detectable for $0.1\lesssim V_G\lesssim0.2$ V. At lower values of $B$, structure in the derivative curves is not resolved. Similar structure is observed for $I$-$V$ curves between 1.6 and 4.0 K, although the data are noisier at higher temperatures.

In Fig. 6, $\Delta V_m$ for both maxima and minima is plotted (circles) as a function of $V_G$ for several values of $B$. The value of $V_G$ is the larger of the two voltages used to calculate each $\Delta V_m$. The vertical lines in Fig. 6(e) show $\Delta V_m\pm2$ mV. Since data is taken at 1 mV intervals, there

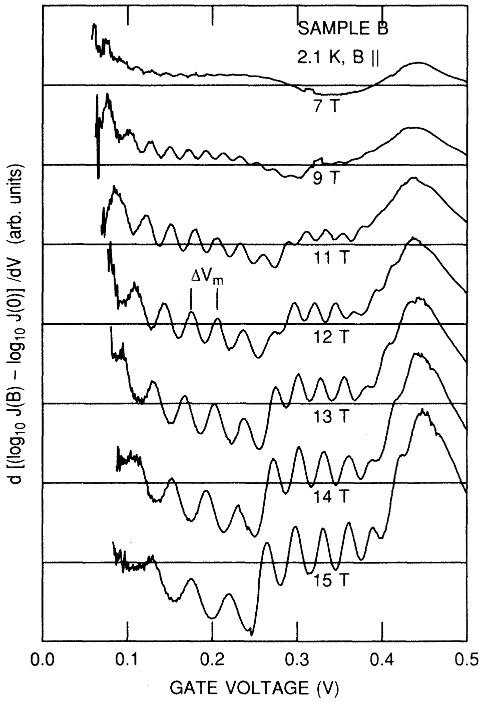

FIG. 5. Derivatives of $[\log_{10}J(B)-\log_{10}J(0)]$ with respect to $V_G$ for different values of $B$ for sample $B$. $\Delta V_m$ is the voltage difference between successive maxima or minima. Curves have the same ordinate scale but are shifted.

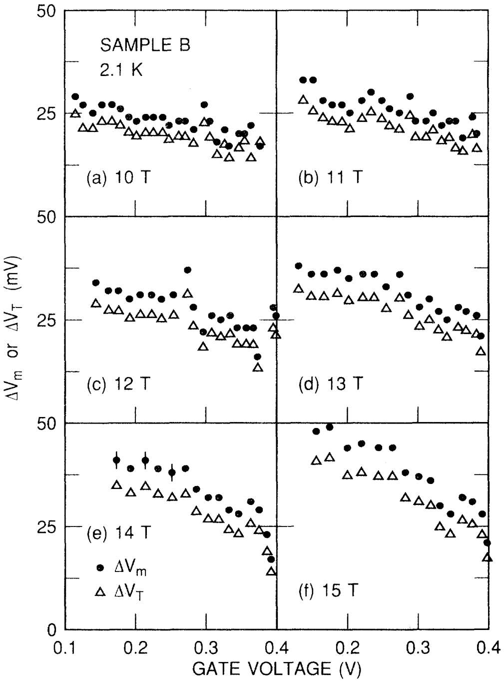

FIG. 6. Dependence on gate voltage of difference in maxima or minima of derivative curves, $\Delta V_m$, and values of $\Delta V_m$ corrected for band bending in gate, $\Delta V_T=(\Delta V_m-\Delta\psi_G)$, at different transverse magnetic fields for sample $B$.

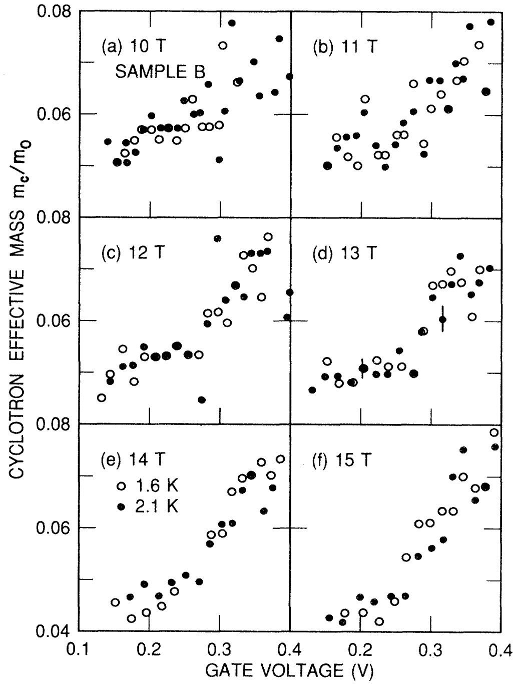

FIG. 7. Dependence on $V_G$ of cyclotron effective mass at $Al_xGa_{1-x}As/(n^+$-type GaAs) interface, $m_c/m_0$, derived from $\Delta V_T$, for different transverse magnetic fields for sample $B$. $T=1.6$ and 2.1 K.

is an estimated error of 1 or 2 mV for any point. Within experimental error, $\Delta V_m$ is constant for $V_G \lesssim 0.24$ V and $B \geq 10$ T. The constancy of $\Delta V_m$ for $0.3 \lesssim V_G \lesssim 0.4$ V is more easily seen in Fig. 5 than in Fig. 6.

Measurements of $\Delta V_m$ in Fig. 5 correspond closely to the schematic diagram in Fig. 1(b). For low bias, electrons tunnel from $n^-$-type GaAs into Landau states below the barrier at the $Al_xGa_{1-x}As/(n^+$-type GaAs) interface. For higher biases, they tunnel into states above the $Al_xGa_{1-x}As$/GaAs band discontinuity. To make this relation more quantitative it is necessary to correct for band bending in the $n^+$-type GaAs gate $\Delta\psi_G$. This has been done using $V_T$ in Fig. 2(b). For each value of $\Delta V_m$ there is a corrected value $\Delta V_T$, which is plotted as triangles in Fig. 6. Just as $qV_T$ is the energy of electrons above the conduction-band edge at the $Al_xGa_{1-x}As$/GaAs interface as they tunnel into $n^+$-type GaAs, $q\Delta V_T$ is the change in energy at the $Al_xGa_{1-x}As$/GaAs barrier corresponding to each value of $\Delta V_m$. The correction is a significant one.

According to Ref. 6, each maximum in the derivative curve results from the opening of a new tunneling channel. Correspondingly, if $\Delta V_T$ equals the separation of Landau states at the interface, values of $\Delta V_T$ can be used to calculate a cyclotron effective mass $m_c$ for electrons at the $Al_xGa_{1-x}As/(n^+$-type GaAs) interface. For bulk GaAs, $m_e=0.067m_0$ at the conduction-band edge, where $m_0$ is the free-electron mass, which gives $\hbar\omega_c=1.728B$ meV as the spacing between bulk Landau levels. For Landau levels at an infinite barrier, the spacing is $2\hbar\omega_c$, which would correspond to $m_c=0.034m_0$. In Fig. 7, values of $q\Delta V_T$ in Fig. 6 are taken equal to $\hbar\omega_c$ at the $Al_xGa_{1-x}As/(n^+$-type GaAs) interface. They have been converted to values of $m_c$ using the relation

$$m_c=\frac{\hbar qB}{q\Delta V_T}=\frac{0.1158B(\mathrm{T})}{\Delta V_T(\mathrm{mV})}\ , \qquad (3)$$

which is derived from Eq. (1). Values of $m_c$ are shown for data taken at 1.6 and 2.1 K. The vertical bars for two points at 13 T show the effect of a ±1 mV error in $\Delta V_m$ on $m_e$. Within experimental error, $m_c$ is constant for $0.1 \lesssim V_G \lesssim 0.24$ V. There is then a steep rise in $m_c$, and for $V_G \sim 0.4$ V, $m_c$ is between 0.07 and 0.08, which approaches the interpolated value for the effective mass for electrons in $Al_{0.3}Ga_{0.7}As$, $m_e/m_0=0.09$. Transverse magnetotunneling requires that both energy and transverse momentum be conserved. In equating $\hbar\omega_c$ and $qV_T$, it is assumed that the density of states at the interface between $Al_xGa_{1-x}As$ and $n^+$-type GaAs is large enough that transverse momentum can be conserved for all energies.

Similar results are obtained for sample $A$, but there are significant differences in detail. Figure 8 shows derivative curves for sample $A$ at different magnetic fields. Because of the thicker and higher barrier, currents are lower and a larger range of gate voltages can be explored. Structure in the derivative curve can be resolved at 8 T; it is visible

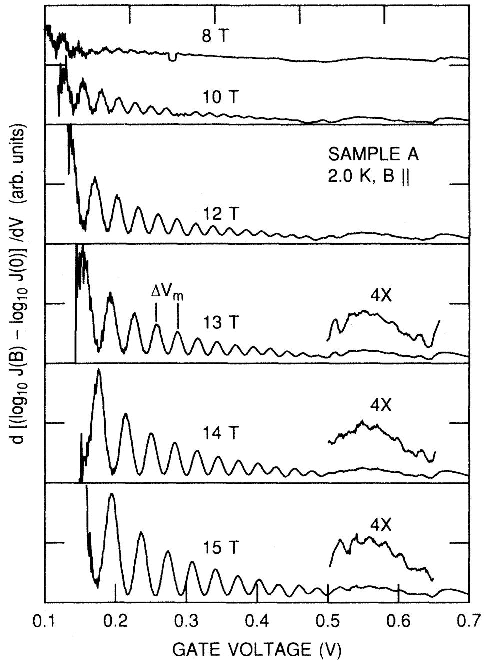

FIG. 8. Derivatives of $[\log_{10}J(B)-\log_{10}J(0)]$ with respect to $V_G$ for different values of $B$ for sample $A$. $\Delta V_m$ is the voltage difference between successive maxima or minima. Curves have the same ordinate scale but are shifted.

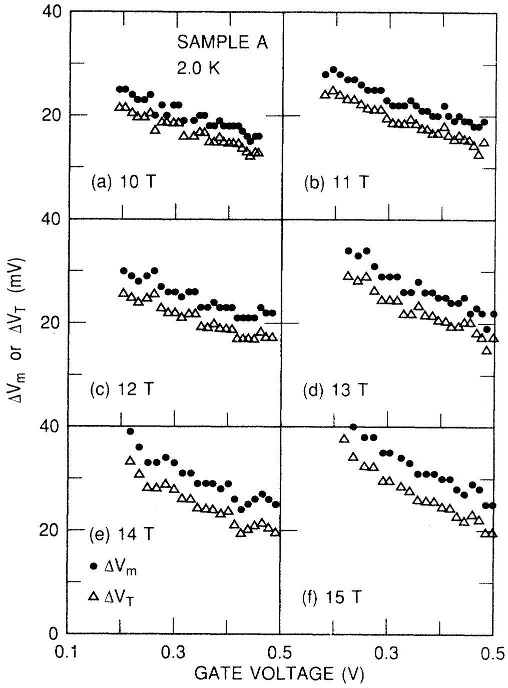

FIG. 9. Dependence on gate voltage of difference in maxima or minima of derivative curves, $\Delta V_m$, and values of $\Delta V_m$ corrected for band bending in gate, $\Delta V_T=(\Delta V_m-\Delta\psi_G)$, at different transverse magnetic fields for sample $A$.

at 7 T but not at 6 T. For curves from 13 to 15 T structure between 0.5 and 0.65 V is shown at 4× magnification. Even at such high biases, modulation of $I$-$V$ curves can be detected. Solid lines in Fig. 8 correspond to zero for derivative curves.

Values of $\Delta V_m$ and $\Delta V_T$ for sample $A$ are shown in Fig. 9. Parameters used for modeling $C$-$V$ curves and for obtaining $\Delta V_T$ for sample $A$ are given in Table I. In contrast to sample $B$, there is no voltage range of constant $\Delta V_m$; instead, there is a gradual decrease of $\Delta V_m$ or $\Delta V_T$ as $V_G$ increases. Cyclotron effective masses derived from $\Delta V_T$ measured at 1.6 and 2.0 K are shown in Fig. 10. The variation of $m_c$ is nearly linear in $V_G$. The lowest values are about the same as for sample $B$, but the largest values approach that expected for $Al_{0.4}Ga_{0.6}As$, $m_e/m_0=0.10$. Data between 0.5 and 0.65 V in Fig. 8 are now well resolved; however, for $B=15$ T, $m_c/m_0=0.10$ at $V_G\sim0.55$ V.

For both samples $A$ and $B$, tunneling at low bias is direct tunneling; electrons tunnel through the whole thickness of the undoped $Al_xGa_{1-x}As$ and enter the $n^+$-type GaAs at an energy less than the barrier height at the $Al_xGa_{1-x}As/(n^+$-type GaAs) interface, which is due to the band discontinuity between the two semiconductors. In Fig. 11, $\Delta V_m$ and $\Delta V_T$ for the two samples at $V_G\simeq0.2$ V are plotted as a function of magnetic field. The solid line is the cyclotron energy for the effective mass at the GaAs band edge, $0.067m_0$, as a function of $B$.

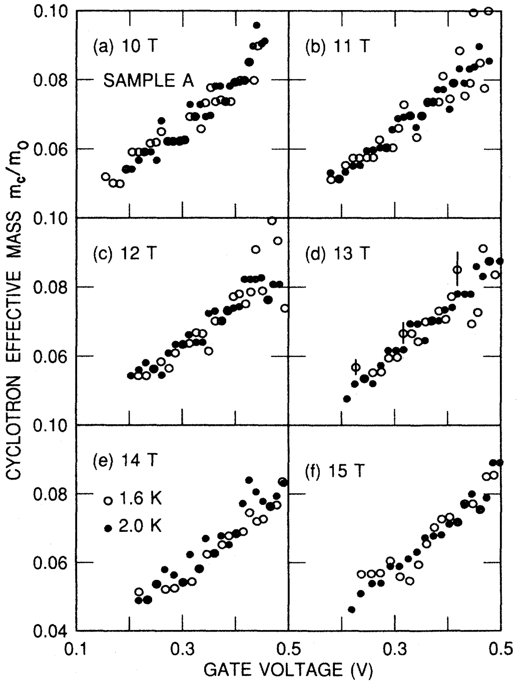

FIG. 10. Dependence on $V_G$ of cyclotron effective mass at $Al_xGa_{1-x}As/(n^+$-type GaAs) interface, $m_c/m_0$, derived from $\Delta V_T$, for different transverse magnetic fields for sample $A$. $T=1.6$ and 2.0 K.

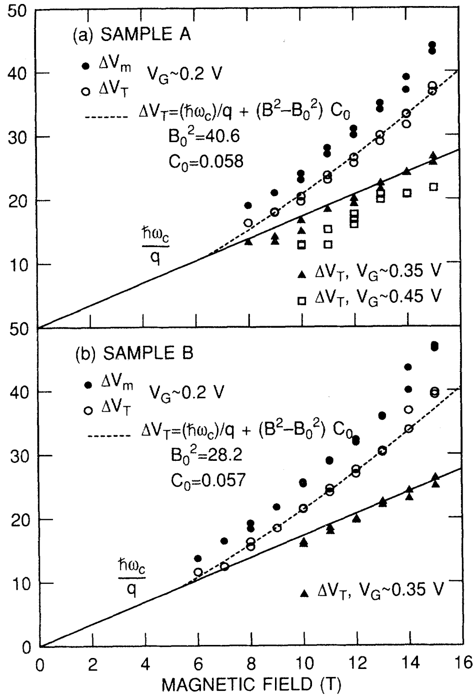

FIG. 11. Dependence of $\Delta V_m$ and $\Delta V_T$ at ~0.2 V, and of $\Delta V_T$ at other values of $V_G$, on transverse magnetic field for sample $A$ and for sample $B$. Solid line is Landau-level spacing for $m_e = 0.067 m_0$. Dotted line is parabolic fit to data at $V_G \sim 0.2$ V.

The dotted line is a least-squares parabolic fit of $V_T$ against $B$:

$$\Delta V_T = (\hbar\omega_c / q) + (B^2 - B_0^2) C_0 . \tag{4}$$

Several values of $\Delta V_T$ around 0.2 V were averaged to obtain the values plotted for sample $B$; for sample $A$, the extrema closest to $V_G = 0.2$ V were used. Although the derivative curves for the two samples differ significantly, the value of $C_0$ is the same. $B_0^2$ is smaller for sample $B$. Thus the separation of Landau levels for energies less than the band discontinuity at the $\mathrm{Al}_x\mathrm{Ga}_{1-x}\mathrm{As}/(n^+$-type GaAs) interface is not a simple linear function of $B$. The origin of the component parabolic in $B$ is not clear. Also shown in Fig. 11(a) are $\Delta V_T$ at $V_G \simeq 0.35$ V and $V_G \simeq 0.45$ V. The former are close to the line for the cyclotron energy corresponding to $m_e = 0.067 m_0$; the latter have an energy that is lower. In Fig. 11(b), values of $V_T$ at $V_G \simeq 0.35$ V are also slightly lower than the cyclotron energy for $m_e = 0.067 m_0$.

### Tunneling at constant gate bias

The complementary measurements to $I$-$V$ curves at constant magnetic field, such as those in Fig. 3, is to hold $V_G$ constant and measure $I$ while sweeping the magnetic field. In such measurements ($I$-$V$-$B$ curves) the surface concentration in the accumulation layer is approximately constant, and a sequence of Landau states moves past the energy $qV_T$ at which electrons tunnel into the $\mathrm{Al}_x\mathrm{Ga}_{1-x}/(n^+$-type GaAs) interface. Figure 12 shows $I$-$V$-$B$ curves for both samples in which $J(B)/J(0)$ is plotted as a function of $B$ at constant $V_G$. Both samples show a marked drop in current as $B$ increases. For sample $A$, the drop is monotonic in $B$ at all biases. There is an approximately invariant value of $J(B)/J(0)$ at ~5.6 T. Its origin is uncertain, but the value of $B$ is that for which the cyclotron orbit diameter of electrons equals the barrier thickness. For sample $B$, the drop is monotonic for $0.1 \lesssim V_G \lesssim 0.33$ V. For $V_G \gtrsim 0.34$ V there is a small increase in $J(B)/J(0)$ for $B \lesssim 4$ T. Such an increase in $J(B)/J(0)$, characteristic of the effect of a transverse magnetic field on resonant Fowler-Nordheim tunneling in $\mathrm{Al}_x\mathrm{Ga}_{1-x}\mathrm{As}$ capacitors, arises from the change of electron phase in a transverse magnetic field.[19] A phase change of electrons that tunnel into the $\mathrm{Al}_x\mathrm{Ga}_{1-x}\mathrm{As}$ conduction band when $V_G$ exceeds $\phi_G$ modifies electron interference, which helps determine the shape of $I$-$V$ curves of sample $B$. In both samples modulation of $I$-$V$-$B$ curves can be seen for $B \gtrsim 10$ T. Guéret, Baratoff, and Marclay[23] have studied transverse magnetotunneling in $n^+$-type GaAs–undoped $\mathrm{Al}_x\mathrm{Ga}_{1-x}\mathrm{As}$–$n^+$-type GaAs capacitors with low, wide barriers. For $B < 4$ T they find that the decrease in $J$ at constant $V_G$ is proportional to $B^2$. The present work uses samples with higher, thinner barriers and a wider range of $B$. In such a case the behavior of $J(B)/J(0)$ is more complex than a simple decrease proportional to $B^2$.

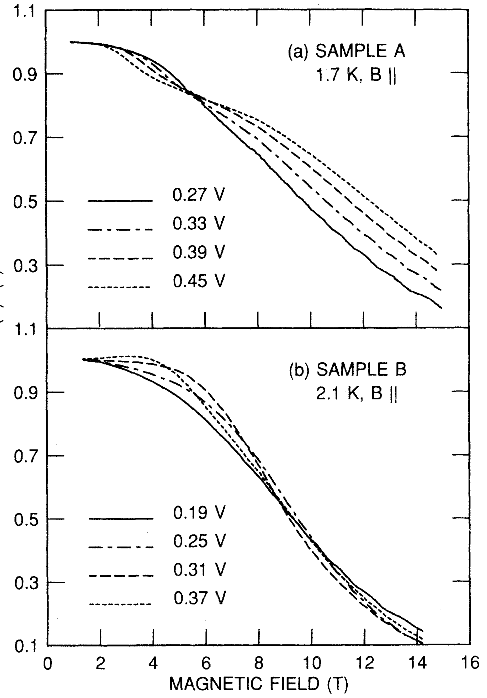

FIG. 12. Dependence of the ratio of current density at magnetic field $B$ and constant $V_G$ to current density at zero magnetic field at $V_G$ on magnetic field for samples $A$ and $B$.

Structure in *I-V-B* curves is clearly shown by taking derivatives with respect to $B$. Data for sample $A$ are shown in Fig. 13 and for sample $B$ in Fig. 14. Structure is seen in derivative curves for $B \gtrsim 7$ T at lower values of $V_G$, which is consistent with *I-V* curves. For sample $A$, no structure is resolved for $V_G \gtrsim 0.50$ V; for sample $B$, no structure is resolved for $V_G \gtrsim 0.42$ V. For bulk GaAs the energy dispersion of Landau levels is given by Eq. (1). If Eq. (1) is valid for electrons tunneling at the $\mathrm{Al}_x\mathrm{Ga}_{1-x}\mathrm{As}/(n^+$-type GaAs) interface, a plot of $N$ versus $1/B$ should be linear, and an effective cyclotron mass is given by

$$m_c = \frac{\hbar q B}{(E_T - E_C)\dfrac{dN}{d(1/B)}} , \qquad (5)$$

where $E_T - E_C$ is the energy of an electron above the conduction-band edge at the $\mathrm{Al}_x\mathrm{Ga}_{1-x}\mathrm{As}/(n^+$-type GaAs) interface.

Figure 15 plots the Landau level index $N$ as a function of $10/B$ for maxima of the derivative curves of Fig. 13 or 14. Solid lines are least-squares fits of the experimental data. A similar plot can be made for minima in the derivatives. $N$ is proportional to $1/B$ for both maxima and minima. In Fig. 16, values of $dN/d(1/B)$ are given for maxima and minima of both samples for different gate voltages. The lines are a linear least-squares fit of the data. Within the spread of the data, the linear fit is valid. Using the data of Fig. 16, values of $m_c$ as a function of $V_G$ are given in Fig. 17. $E_T - E_C$ is obtained from calculated *C-V* curves as in Fig. 2(b).

Values of $m_c$ calculated from Eq. (5) are less than $m_e$

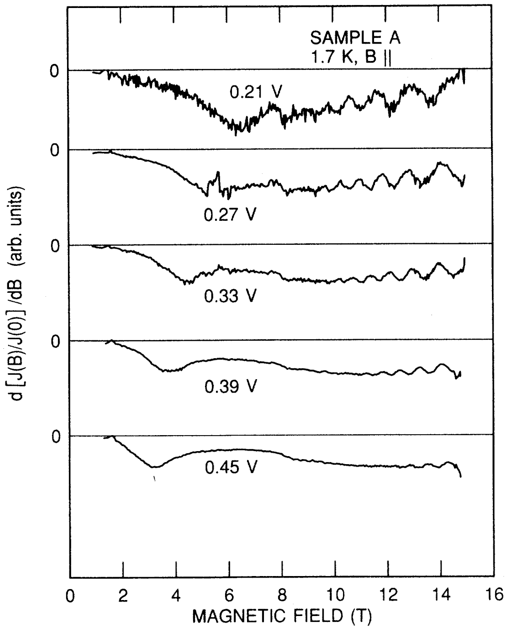

FIG. 13. Derivative of $J(B)/J(0)$ with respect to $B$ at constant values of $V_G$ for *I-V-B* curves for sample $A$.

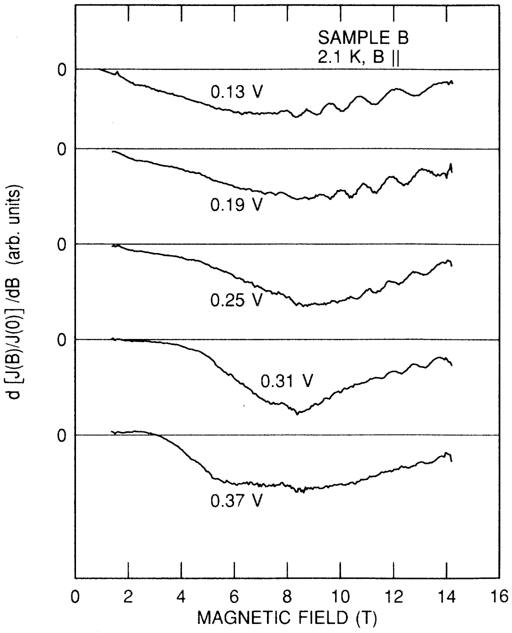

FIG. 14. Derivative of $J(B)/J(0)$ with respect to $B$ at constant values of $V_G$ for *I-V-B* curves for sample $B$.

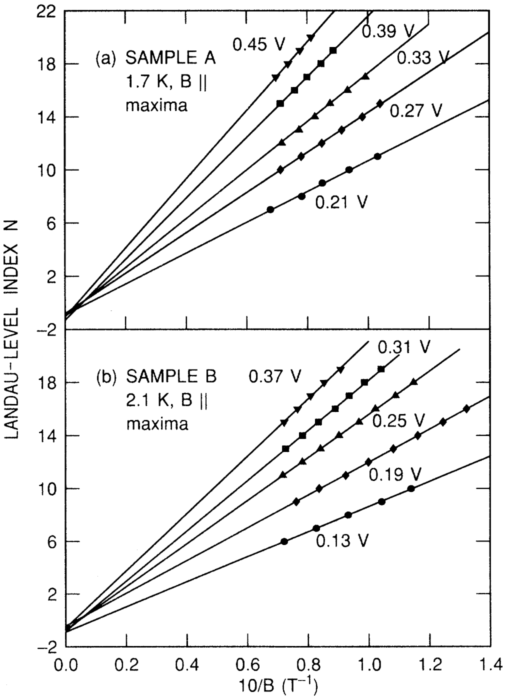

FIG. 15. Dependence of Landau level index $N$ of maxima in $d[J(B)/J(0)]/dB$ on $1/B$ at constant $V_G$ for *I-V-B* curves for samples $A$ and $B$.

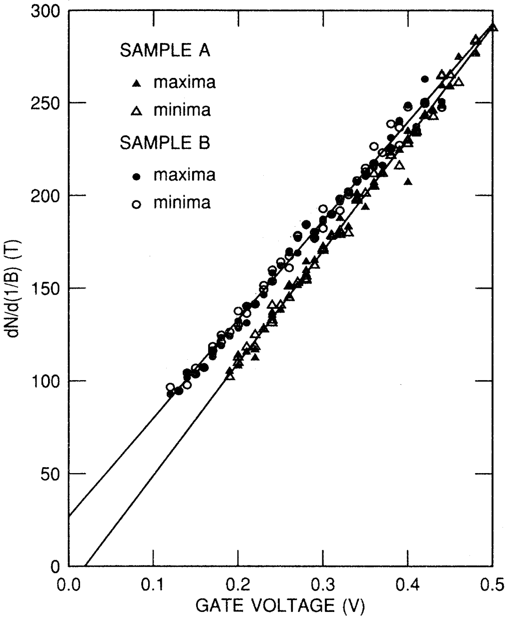

FIG. 16. Dependence of maxima and minima of $dN/d(1/B)$ for samples $A$ and $B$ on $V_G$.

for GaAs at low bias and greater than $m_e$ at high bias, but the range is not as great as in Fig. 7 or 10, where $m_c$ is obtained from $I$-$V$ curves. There are several possible reasons. Extrema for derivative curves such as in Fig. 15 or 16 are less accurately determined than extrema for derivative curves such as in Fig. 5 or 8. Calculating $m_c$ from Eq. (5) requires knowledge of the absolute value of $E_T - E_C$, while the values of $m_c$ in Fig. 7 or 10 require an estimate of $\Delta\psi_G$ for a relatively small change in $V_G$, $\Delta V_m$. The latter is more accurately determined. At low bias, Fig. 11 shows there is a parabolic dependence of $\Delta V_T$ on $B$ for $V_G$ in the direct tunneling regime, though the relation is nearly linear when $V_G$ is greater than the value required for FN tunneling. No parabolic dependence of the spacing of Landau states is included in Eq. (5), and this can introduce errors at low bias. In spite of uncertainties in the value of $m_c$, the proportionality of $N$ and $1/B$ is observed.

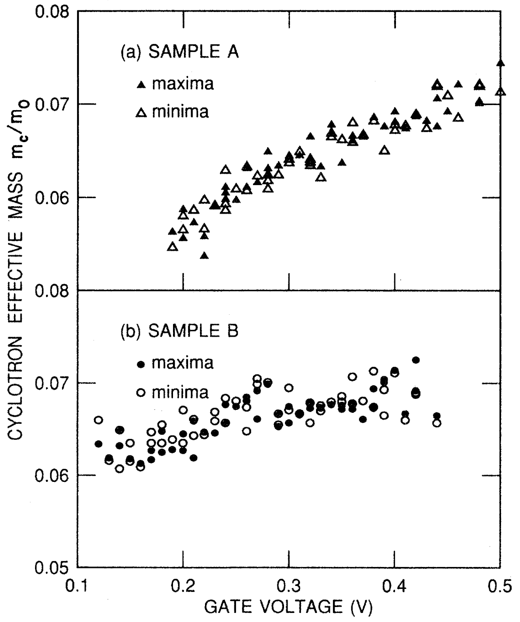

FIG. 17. Dependence of $V_G$ of cyclotron effective mass at $Al_xGa_{1-x}As/(n^+$-type GaAs) interface, $m_c$, derived from extrema of derivatives of $I$-$V$-$B$ curves.

## DISCUSSION

Theoretical calculations[6-9] have shown that structure is expected to occur in transverse magnetotunneling $I$-$V$ curves for single-barrier heterostructures. Each time the Fermi energy of electrons in the accumulation layer in the $n^-$-type GaAs source equals the energy of an interface Landau state in the $n^+$-type GaAs gate, a new channel for tunneling opens and affects the tunneling current.

Likewise, calculations of the nature and spacing of interface Landau states in a transverse magnetic field have shown the complexity of allowed electron states in crossed electric and magnetic fields.[15-17] The schematic diagram of Fig. 1(b) suggests that the spacing and nature of Landau states below the band discontinuity $V_0$ differs from those above the band discontinuity. However, quantitative comparison with experiment is not possible, since $V_0$ in Fig. 1(b) is lower than the band discontinuity in the $Al_xGa_{1-x}As$ capacitors studied. In addition, the layers with effective mass $m_1$ and $m_2$ in Fig. 1(b) are assumed to be infinite;[17] in the samples studied, the $Al_xGa_{1-x}As$ barrier has finite thickness which is comparable to or greater than magnetic lengths for $B > 6$ T.

Experimental results that show structure in transverse magnetotunneling curves of single-barrier heterostructures are less extensive than calculations. For $n^-$-type (In,Ga)As–undoped InP–$n^+$-type (In,Ga)As (InP) capacitors, two distinct series of resonances are observed in transverse magnetotunneling curves.[2-5] Magnetic fields as low as 2 T modulate $I$-$V$-$B$ curves. Snell *et al.*[2] have explained the occurrence of two series on the basis that one series corresponds to electrons that tunnel with $k_y = +k_F$, and the other corresponds to electrons that tunnel with $k_y = -k_F$, where $k_F$ is the wave vector of electrons at the Fermi level of the accumulation layer and $k_y$ is the electron wave vector in the direction perpendicular to both $J$ and $B$. By contrast, only one series of peaks due to interface states is observed in the derivative of $I$-$V$ curves of $n^-$-type GaAs–undoped $Al_xGa_{1-x}As$–$n^+$-type GaAs capacitors, and it is not observed for $B \lesssim 6$ T. Fromhold, Sheard, and Toombs[9] attribute this series to electrons in the accumulation layer for which $k_y = -k_F$; the series for electrons with $k_y = +k_F$ does not occur. They suggest that this is due to the greater barrier thickness for sample $A$ than for their InP capacitor. However, the tunneling thickness of sample $B$ is closer to that of their InP capacitor, and only a single series of extrema is observed.

The fact that only a single series of extrema occurs in the $Al_xGa_{1-x}As$ capacitors enables one to map the spacing of interface states at the $Al_xGa_{1-x}As/(n^+$-type GaAs) interface. Such a schematic map for $B=15$ T is shown in Fig. 18(a) for sample $A$ and in Fig. 18(b) for sample $B$. In each figure, $V_T$, calculated from $C$-$V$ curves, is plotted on one axis. On the right axis $E_T=qV_T$ is given as multiples of $\hbar\omega_c$ for $B=15$ T and $m_e=0.067m_0$; $\hbar\omega_c=25.92$ meV at 15 T. The minimum value of $E_T/\hbar\omega_c$ is 6 in each part of the figure, since lower Landau levels are not probed in either sample. $E_C$, which is equivalent to $V_0$ in Fig. 1(b), shows the position of the band discontinuity at the $Al_xGa_{1-x}As/(n^+$-type GaAs) interface in units of $\hbar\omega_c$. The energy axis $qV_{\max}$ shows the position of maxima of the derivatives in Figs. 6 and 9 in units of $\hbar\omega_c$. The voltage scale $V_G$ is the gate voltage which corresponds to $V_T$ and $V_{\max}$. For both samples there is a noticeable decrease of the spacing $qV_{\max}$ when $E_T>V_0$. For sample $B$, the value of $V_G$ for which tunneling is above $E_C$ corresponds closely to the transition between the two regions with different period in Fig. 5. For $E_T\lesssim V_0$ the spacing of maxima is greater than $\hbar\omega_c$; for $E_T\gtrsim V_0$, the spacing is less than $\hbar\omega_c$. Since Fig. 18 is for a single value of $B$, it does not show the parabolic dependence on $B$ which is found in Fig. 11. For both samples, electrons are tunneling at energies that are several hundred meV above $E_C$. Nonparabolicity of the conduction band also contributes to a decrease in spacing of extrema at higher biases and would need to be considered in a quantitative theory.

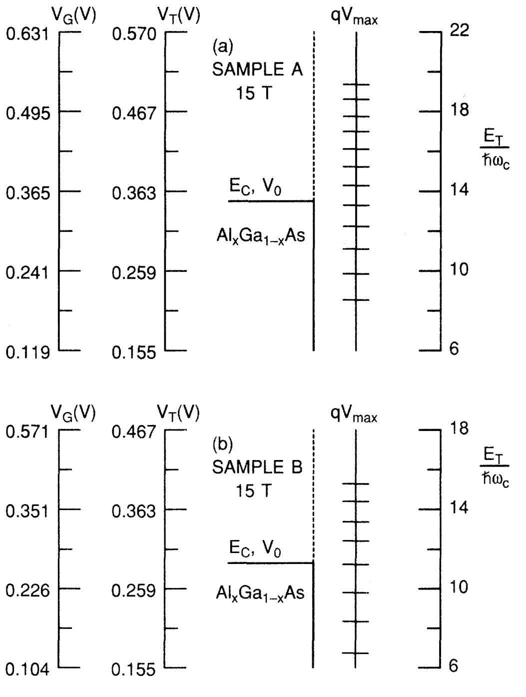

FIG. 18. Schematic diagram of the spacing of Landau states at the $Al_xGa_{1-x}As/(n^+$-type GaAs) interface for samples $A$ and $B$ in a transverse magnetic field of 15 T.

$I$-$V$-$B$ curves such as those in Fig. 12 have been calculated using a transfer Hamiltonian method.[6-8] The parameters of the calculation correspond closely to those of sample $A$. The authors find that the positions of extrema should be proportional to $1/B$, as in Fig. 15. They calculate tunnel currents as a function of $1/B$ for $V_G=0.4$ V, which is close to the value $V_G=0.39$ V in Figs. 12, 13, and 15. They find four maxima for $1/B$ between 0.07 and 0.09, which does not agree quantitatively with five maxima observed for $0.07\leq 1/B\leq 0.09$ $T^{-1}$ in Fig. 15. Tunneling at $V_G=0.4$ V is into states above the barrier at the $Al_xGa_{1-x}As/(n^+$-type GaAs) interface; their calculation does not take account of the narrowing of the spacing of Landau states in that energy region.

Both $Al_xGa_{1-x}As$ capacitors that show structure in transverse magnetotunneling curves, samples $A$ and $B$, have barriers that are thin enough that direct tunneling occurs. In Ref. 19, transverse magnetotunneling was studied in two samples that are about 10 nm thicker and that show resonant FN tunneling. $I$-$V$ curves could not be measured until $V_G$ exceeded the magnitude of the barrier at the $Al_xGa_{1-x}As/(n^+$-type GaAs) interface. In both samples the transverse magnetic field modulated $I$-$V$ curves by changing the phase of electrons that tunnel into $Al_xGa_{1-x}As$ and are reflected at the $Al_xGa_{1-x}As/(n^+$-type GaAs) interface. However, neither sample showed structure in $I$-$V$ curves such as in Fig. 5 or 8, nor did $I$-$V$-$B$ curves, such as in Fig. 13 or 14, show similar structure. For sample $B$, the curve for $V_G=0.37$ V in Fig. 12(b) shows that resonant FN tunneling contributes to $I$-$V$ curves, so the occurrence of FN tunneling does not necessarily destroy structure due to tunneling into interface states. The reason for the lack of structure in the thicker samples is not known but may be related to the fact that all electrons contributing to $I$-$V$ curves tunnel into $Al_xGa_{1-x}As$ before being collected in the $n^+$-type GaAs layer.

The emphasis in the present work is on the structure in transverse magnetotunneling curves of single-barrier heterostructures due to tunneling into Landau states at the $Al_xGa_{1-x}As/(n^+$-type GaAs) interface. Several other recent papers have been concerned with transverse magnetotunneling in single-barrier heterostructures. Magnetotunneling between two independently contacted 2DEG systems separated by a barrier has been studied in $GaAs/Al_xGa_{1-x}As$ heterostructures.[24-26] The authors attribute structure in $I$-$V$ curves at 0 T to tunneling into subbands of the 2DEG that forms one interface of their heterostructure. They show transverse momentum conservation in their system. Lebens, Silsbee, and Wright,[27,28] using measurements of ac conductance of electrons tunneling between a quantum well and an $n^+$-type GaAs electrode, have also shown that transverse momentum is conserved in transverse magnetotunneling.

In conclusion, transverse magnetotunneling curves have been measured at 1.6–4.0 K on two $Al_xGa_{1-x}As$

capacitors which have dielectric $Al_xGa_{1-x}As$ layers thin enough that direct tunneling occurs at low bias. Both $I$-$V$ curves at constant $B$ and variable $V_G$, and $I$-$V$-$B$ curves at constant $V_G$ and variable $B$, show structure due to tunneling into magnetic Landau states at the $Al_xGa_{1-x}As/(n^+$-type GaAs) interface. Capacitance-voltage curves are used to correct the spacing of extrema in $I$-$V$ and $I$-$V$-$B$ curves for band bending in the gate electrode. Values of the corrected voltage spacings are converted to cyclotron effective masses for electrons at the $Al_xGa_{1-x}As/(n^+$-type GaAs) interface; $m_c/m_0$ varies from 0.042 at low bias to 0.10 for high biases in which electrons tunnel into $Al_xGa_{1-x}As$ before being collected in the $n^+$-type GaAs gate. Although $I$-$V$ curves of both samples show structure in transverse magnetotunneling curves, there are differences in behavior that depend on detailed differences in the sample structures.

## ACKNOWLEDGMENTS

Magnetic-field measurements were made through the courtesy of F. F. Fang. Sample $A$ was provided by H. Morkoç and sample $B$ by S. L. Wright. I have benefited from conversations with F. Stern. E. Mendez and F. Stern have read and commented on the manuscript.

---

[1] T. W. Hickmott, Solid State Commun. **63**, 371 (1987).

[2] B. R. Snell, K. S. Chan, F. W. Sheard, L. Eaves, G. A. Toombs, D. K. Maude, J. C. Portal, S. J. Bass, P. Claxton, G. Hill, and M. A. Pate, Phys. Rev. Lett. **59**, 2806 (1987).

[3] F. W. Sheard, L. Eaves, and G. A. Toombs, Phys. Scr. **T19**, 179 (1987).

[4] F. W. Sheard, K. S. Chan, G. A. Toombs, L. Eaves, and J. C. Portal, in *Proceedings of the 14th International Symposium on GaAs and Related Compounds,* edited by A. Christou and H. S. Rupprecht, IOP Conf. Proc. No. 91 (Institute of Physics, London, 1987), p. 387.

[5] K. S. Chan, L. Eaves, D. K. Maude, F. W. Sheard, B. R. Snell, G. A. Toombs, E. S. Alves, J. C. Portal, and S. Bass, Solid-State Electron. **31**, 711 (1988).

[6] L. Brey, G. Platero, and C. Tejedor, Phys. Rev. B **38**, 9649 (1988).

[7] P. A. Schulz and C. Tejedor, Phys. Rev. B **39**, 11 187 (1989).

[8] G. Platero, P. A. Schulz, L. Brey, and C. Tejedor, Surf. Sci. **228**, 291 (1990).

[9] T. M. Fromhold, F. W. Sheard, and G. A. Toombs, Surf. Sci. **228**, 437 (1990).

[10] T. W. Hickmott, Phys. Rev. B **32**, 6531 (1985).

[11] E. Böckenhoff, K. v. Klitzing, and K. Ploog, Phys. Rev. B **38**, 10 120 (1988).

[12] K. S. Chan, F. W. Sheard, G. A. Toombs, and L. Eaves, Superlatt. Microstruct. **9**, 23 (1991).

[13] T. Ando, A. B. Fowler, and F. Stern, Rev. Mod. Phys. **54**, 437 (1982).

[14] J. P. Vigneron and M. Ausloos, Phys. Rev. B **18**, 1464 (1978).

[15] J.-K. Maan, in *Festkörperprobleme (Advances in Solid State Physics),* edited by P. Grosse (Vieweg, Braunschweig, 1987), Vol. 27, p. 137.

[16] E. A. Johnson, A. MacKinnon, and C. J. Goebel, J. Phys. C **20**, L521 (1987).

[17] E. A. Johnson and A. MacKinnon, J. Phys. C **21**, 3091 (1988).

[18] T. W. Hickmott, Phys. Rev. B **40**, 8363 (1989) (paper I).

[19] T. W. Hickmott, Phys. Rev. B **40**, 11 683 (1989) (paper II).

[20] T. W. Hickmott, Phys. Rev. B **38**, 12 404 (1988).

[21] T. W. Hickmott, P. M. Solomon, R. Fischer, and H. Morkoç, J. Appl. Phys. **57**, 2844 (1985).

[22] $C$-$V$ curves at low temperature were calculated with a computer program provided by F. Stern. It is a continuum model that includes no quantum effects.

[23] P. Guéret, A. Baratoff, and E. Marclay, Europhys. Lett. **3**, 367 (1987).

[24] J. Smoliner, E. Gornik, and G. Weimann, Phys. Rev. B **39**, 12 937 (1989).

[25] J. Smoliner, W. Demmerle, G. Berthold, E. Gornik, G. Weimann, and W. Schlapp, Phys. Rev. Lett. **63**, 2116 (1989).

[26] W. Demmerle, J. Smoliner, G. Berthold, E. Gornik, G. Weimann, and W. Schlapp, Surf. Sci. **229**, 169 (1990).

[27] J. Lebens, R. H. Silsbee, and S. L. Wright, Appl. Phys. Lett. **51**, 840 (1987).

[28] J. Lebens, R. H. Silsbee, and S. L. Wright, Phys. Rev. B **37**, 10 308 (1988).